LOAD-DISPLACEMENT BEHAVIOR OF SINGLE PILE IN SAND USING PHYSICAL MODEL TEST AND FINITE ELEMENT METHOD

*Kamol Amornfa[1] and Nitirach Sa-nguanduan[2]

[1]Department of Civil Engineering, Faculty of Engineering at Kamphaeng Saen, Kasetsart University, Thailand; [2]Department of Irrigation Engineering, Faculty of Engineering at Kamphaeng Saen, Kasetsart University, Thailand

ABSTRACT: Load-displacement behavior of a pile is one of the key parameters in the foundation design of a high-rise building. This research studied the relationship between the load and displacement of a pile in sand using a physical model test and the finite element method (FEM). Five types of sandy soil, including Bangkok sandy soil, were tested using the physical model test with a pile 1 cm in diameter and 30 cm in penetrated length. The results showed that the relationship between the load and actual pile displacements in all soil types was nonlinear with an elastoplastic-strain hardening pattern. This relationship was expressed using a polynomial function for a displacement in the range 0–20 percent of the pile diameter. For easy use, the relationship can be considered a linear function only in the first stage of displacement (0–10 percent of pile diameter), confirming that linear pile spring stiffness can be reasonably used for the design of the foundation. In addition, the finite element method was used to investigate the effect of various factors on pile spring stiffness. The results showed that pile spring stiffness depended on diameter, length, and modulus of the pile and on the soil modulus. In natural soil, the modulus of soil was related to the soil strength and the pile spring stiffness also depended on the soil strength.

Keywords: Pile, Pile spring stiffness, Physical model test, Finite element method

1. INTRODUCTION

Large infrastructures, such as bridges, elevated highways, expressways, and high-rise buildings, are being constructed, especially in Bangkok and nearby provinces. The soil layer in this area is a thick, soft clay layer alternating with a layer of sand. Therefore, piles must be used as a foundation to support the weight of the high-rise building and to transfer that weight to firmer soil layers at a deeper level. A raft is usually used as a medium for conveying forces from the high-rise building to the piles [1-7]. Parameters describing the behavior of the raft, expressed as its moment and shear, are required to specify the reinforcing steel design, and they are commonly calculated using the plate on springs method, by simulating the raft as a thin plate element and the piles as springs, with the analysis undertaken using a general structural analysis computer program [8]. Pile springs are commonly modeled with linear elastic behavior, with the pile spring stiffness or elastic constant of the pile springs (k_p) being determined based on the load on the pile head per settlement. This can be assessed from the static pile load test results, which are typically performed during actual construction to the approved pile capacity [9,10]. However, the initial design will not be able to utilize pile load test results; this, the designer must estimate the value of k_p from past research abroad [11,12] and piling works in Bangkok [13,14].

Teng [11] suggested that k_p can be obtained using the equations:

$$k_p = \frac{EA}{L} \qquad \text{For end-bearing piles} \qquad (1)$$

$$k_p = 2\frac{EA}{L} \qquad \text{For skin-friction piles} \qquad (2)$$

where E is the elasticity modulus of the pile, A is the pile cross-section area, and L is the pile length.

Kiattivisanchai [13] summarized k_p from 237 static pile load tests of bored piles in Bangkok subsoils as being in the range 0.5–4EA/L with a mean value of 2EA/L, as shown in Fig.1.

Masanou and Amornfa [14] extended the study by Kiattivisanchai [13] and presented k_p as in Fig.2 and Eq. (3):

$$\frac{k_p}{(EA/L)} = -0.195 - 0.020 L \ln D - 0.063 \ln D + 0.059 L \qquad (3)$$

2. RESEARCH SIGNIFICANCE

Study of the precise simulation of piles is still improving. Because the foundations of these infrastructures are large, and the cost of work is high,

proper design is essential, with safe and cost-effective application. Pile simulation research is ongoing, with current studies including physical test experiments [15,16] or finite element methods [7,17]. The objective of this study was to investigate the loading behavior of piles in sand based on physical modeling and the effects of various factors influencing the loading behavior of piles using the finite element method (FEM). This research finding will enhance the understanding of pile behavior in the sand. It can be a reference for future pile analysis and design research.
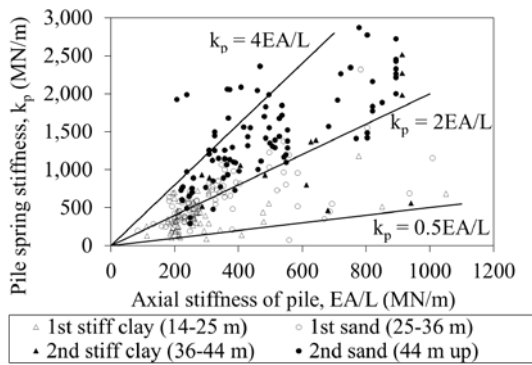

Fig.1 Relationship between axial stiffness and vertical stiffness of bored piles in Bangkok [13]
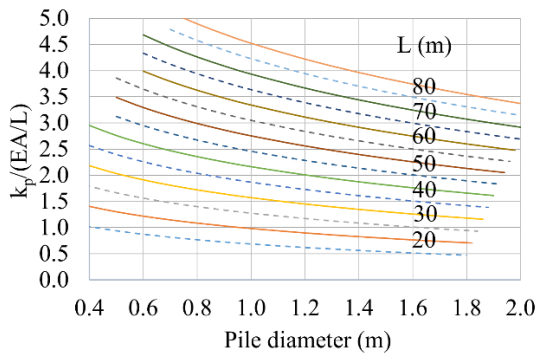

Fig.2 Recommended k_p for bored pile in Bangkok [14]

3. PROPERTIES OF TEST SAMPLE

In this research, five types of sand were used:
- MB: Medium dense sand with gradation the same as Bangkok's first sand layer [18]

- VB: Very dense sand with gradation the same as Bangkok's first sand layer [18]
- MC: Medium dense, coarse sand
- MF: Medium dense, fine sand
- MU: Medium dense uniform sand

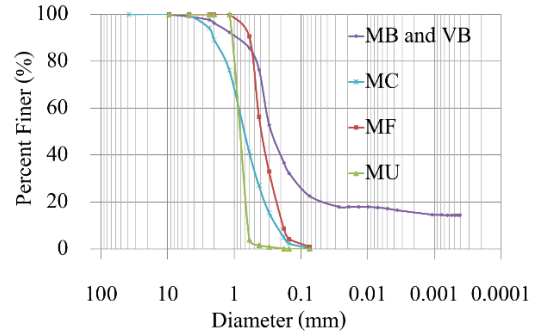The relevant grain size distributions are shown in Fig.3, and other properties are shown in Table 1.

Fig.3 Grain size distribution test results

4. STUDY OF SURFACE FRICTION BETWEEN PILES AND SOIL

Small concrete and soil samples were prepared of the same size as for general direct shear testing. The sample diameter was approximately 7.62 cm (3 inches), and the sample height was about 2.54 cm (1 inch). This study studied concrete samples 1.27 cm (0.5 inches) thick and overlaid with 1.27 cm (0.5 inches) of soil samples. Aluminium samples were also analyzed because aluminium piles were used in the physical modeling tests. Then shear tests were performed on the contact surface using multiple variable vertical weights to measure the shear force and the movement.

Based on the testing results on the contact surface between concrete/aluminium and all five soil types, the angle of friction between pile and soil (δ) was obtained, as shown in Table 2 and Figs.4 and 5. The mean angle of friction between concrete and soil was 0.940 times the angle of internal friction of soil, the mean angle of friction between aluminium and soil was 0.690 times the angle of internal friction of soil and the mean angle of friction between concrete and soil was 1.357 times the angle of friction between aluminium and soil.

Table 1. of soil sample

Soil	Unit	MB	VB	MC	MF	MU
Specific Gravity (G_s)	-	2.69	2.69	2.63	2.68	2.66
Minimum Unit Weight (γ_{min})	g/cm^3	1.514	1.514	1.517	1.366	1.342
Maximum Unit Weight (γ_{max})	g/cm^3	2.005	2.005	1.857	1.686	1.627
Total Unit Weight (γ_t)	g/cm^3	1.725	1.973	1.67	1.51	1.471
Relative density	(%)	50	95	50	50	50
Effective Diameter (D_{50})	mm	0.23	0.23	0.61	0.4	0.82
Fineness Modulus (F.M.)	-	1.41	1.41	2.71	1.72	2.95
Unified Soil Classification (USCS)	-	SM	SM	SP	SP	SP
Internal Friction Angle (ϕ)	°	30.78	36.68	36.54	33.00	32.78

Based on the testing results on the contact surface between concrete/aluminium and all five soil types, the angle of friction between pile and soil (δ) was obtained, as shown in Table 2 and Figs.4 and 5. The mean angle of friction between concrete and soil was 0.940 times the angle of internal friction of soil, the mean angle of friction between aluminium and soil was 0.690 times the angle of internal friction of soil and the mean angle of friction between concrete and soil was 1.357 times the angle of friction between aluminium and soil.

Table 2. Angle of friction between pile and soil

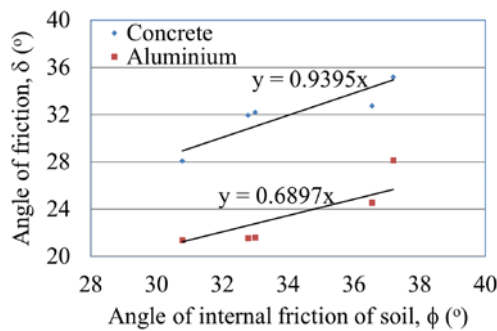| Soil	ϕ (°)	$\delta_{concrete}$ (°)	$\delta_{aluminium}$ (°)
MB	30.78	28.06	21.40
VB	36.68	35.18	28.12
MC	36.54	32.73	24.57
MF	33.00	32.19	21.59
MU	32.78	31.94	21.54

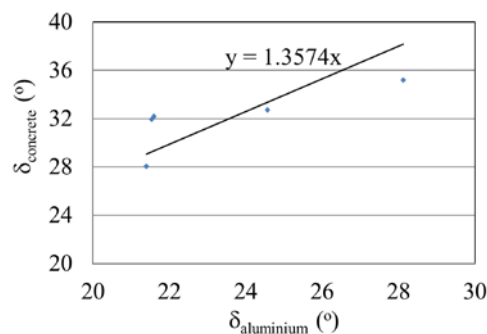Fig.4 Friction angle between pile and soil

Fig.5 Friction angle between aluminium/concrete pile and soil

5. STUDY OF LOADING BEHAVIOR OF PILE IN SAND USING PHYSICAL MODEL TEST

The behavior of pile loading in sandy soil was studied using physical modeling. The model was made in a cylindrical tank with a diameter of 0.59

meters and a soil depth of 0.40 meters, as shown in Figs.6 and 7. Piles with a diameter of 10 millimeters and a pile tip depth of 0.30 meters were installed, with load cells installed at the head of the piles and strain gauges installed at 0, 0.10, 0.20, and 0.30 meters depth.

From the preliminary experiments, casting small concrete piles was difficult because the cross-sectional dimension of the pile was tiny. Thus, casting, ramming fresh concrete in small formwork, and removing the pile from the formwork was problematic, causing the concrete pile to be damaged. In contrast aluminum piles could be purchased easily and were convenient to use. Furthermore, it was more difficult to install strain gauges on the concrete surface because the strain gauges for a concrete surface are large and are unsuitable for simulating smaller piles.
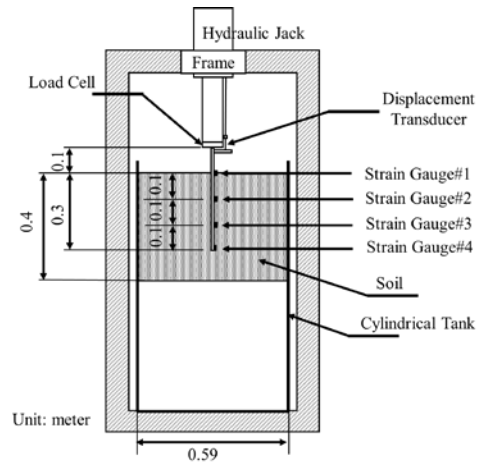

Fig.6 Layout of physical model test

Fig.7 Set up of physical model test

The installation and wiring of the strain gauges are shown in Fig.8. It was found that solid piles with

wiring outside the piles produced measurement inconsistencies due to the relative motion of the piles to the soil. This resulted in tension on the strain gauges, clearly shown by the tension measurement results or wire breakage. In contrast hollow piles were equipped with outer strain gauges and drilled to route the inner cables into the piles, so no tension occurred in measurement and there was less wire damage. Therefore, in the current research, hollow aluminum piles were used to install strain gauge wires inside the piles.

The data of the strain gauges were calculated as the axial force in the piles at various depths. The axial force at a depth of 0 cm was adjusted to the value from the load cell and calculated as the Total pile load. The axial force in piles at depths of 0.10, 0.20, and 0.30 meters were calculated as the friction around the piles at a depth of 0–0.10 meters (Skin friction1), friction around the pile at a depth of 0.10–0.20 meters (Skin friction2), friction around the pile at a depth of 0.20–0.30 meters (Skin friction3) and the axial force at the tip of the pile (End bearing). The calculation results of the five soil types are shown in Figs.9–13.

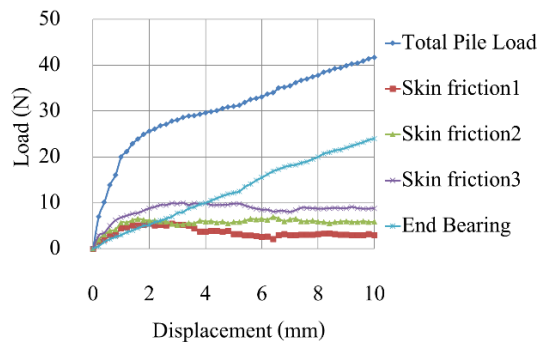Fig.8 Hollow aluminium pile with cable strain gauges inside the pile

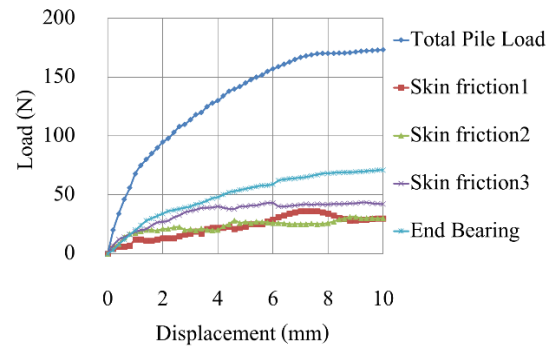Fig.9 Loading behavior of pile in MB soil

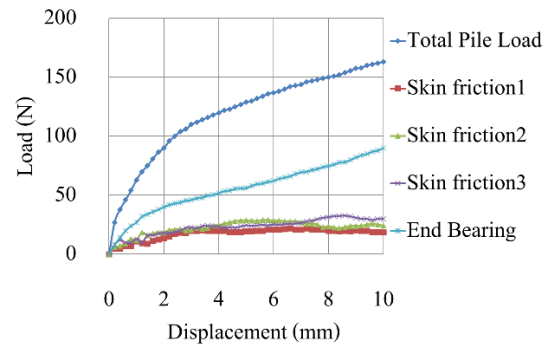Fig.10 Loading behavior of pile in VB soil

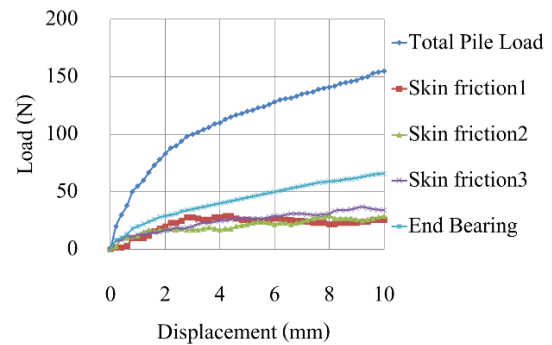Fig.11 Loading behavior of pile in MC soil

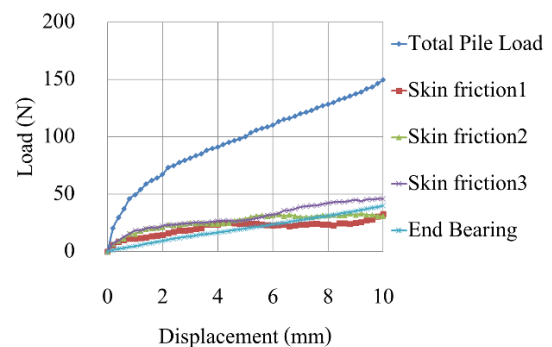Fig.12 Loading behavior of pile in MF soil

Fig.13 Loading behavior of pile in MU soil

From the experimental results of the five soil types, it was found that Skin friction1, Skin friction2, and Skin friction3 were nonlinear with an elastic-perfectly plastic pattern, which is characterized by the initial relationship being elastic

until a displacement of 1–2 mm or 10–20% of the pile diameter and the latter is a plastic relationship with a zero slope. The End bearing is nonlinear with an elastoplastic-strain hardening pattern, characterized by the initial relationship being elastic and then being plastic with a positive slope. The Skin friction1, Skin friction2, Skin friction3, and End bearing were combined to form the Total pile load with a nonlinear relationship with an elastoplastic-strain hardening pattern.

Comparing the Total pile load of the piles in each soil type, the piles in the soil with a higher angle of internal friction were able to carry a greater Total pile load at the same displacement, as shown in Fig.14. In the spring pile foundation simulation, the pile spring stiffness (k_p), as the slope of the curve from the pile displacement in the elastic period was determined in this study from the relationship between the Total pile load and the displacement, only in sections not exceeding 1 mm, which was 10% of the pile diameter. The calculation results for k_p of the piles in each type of soil are shown in Table 3. It was found that the k_p of piles in soil increased with the internal friction angle of the soil.
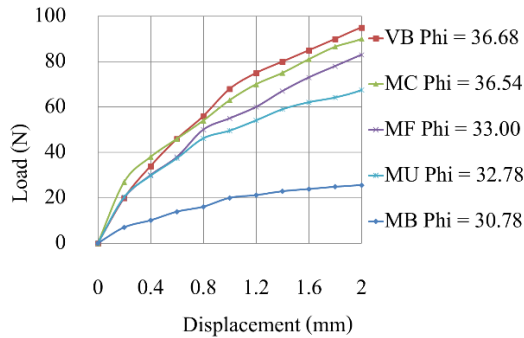

Fig.14 Total pile load for different soils

Table 3. Pile spring stiffness

Soil	ϕ (°)	k_p (N/mm)
VB	36.68	68.0
MC	36.54	63.0
MF	33.00	55.0
MU	32.78	49.6
MB	30.78	20.0

The Total pile load was compared with the ultimate load capacity (Q_u), which was considered at displacement of 0.1 time or 10% of the pile diameter. The relationship is shown in Fig.15. It was found that the five soil types had the same pattern. The nonlinear relationship in the range 0–0.2 of displacement/diameter is shown in Eq. (4):

$$y = 183.33x^3 - 84.866x^2 + 16.682x \quad R^2 = 0.9764 \quad (4)$$

To simplify, the linear relationship in the range of only 0–0.1 of displacement/diameter can be obtained using Eq. (5):

$$y = 10.963x \qquad\qquad R^2 = 0.7875 \quad (5)$$

where x is displacement/diameter, and y is Total pile load/Q_u
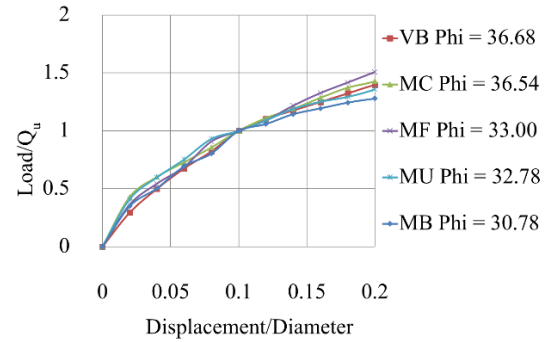

Fig.15 Total pile load/Q_u

6. STUDY OF LOADING BEHAVIOR OF PILES USING FINITE ELEMENT METHOD

The physical modeling study results showed that the load-displacement relationship of the piles increased with the angle of internal friction of the soil. However, because in the laboratory experiments, changing pile sizes and lengths is difficult and costly, the finite element method using the PLAXIS program was applied to find the load-displacement relationship in the pile that changed according to the pile size and length. In addition, the effect of changing soil properties was studied.

In the PLAXIS program, axisymmetrical modeling and a homogeneous soil layer model were simulated at a depth of 0–40 centimeters and a width of 28 centimeters. Mohr-Coulomb elastic-perfectly plastic parameters of MB soil was used as the default. The simulated piles into the soil layer using the linear elasticity material model are shown in Fig.16, with the properties of the piles and soil layers change, according to Table 4.

The results of the finite element analysis are shown in Figs.17–21. When the pile size changed, the slope of the curve changed. Increases in the pile diameter, pile length, pile modulus all resulted in increases in k_p. However, the increase was only small when the pile modulus was high, indicating that the k_p calculation must consider the diameter, length, and modulus of the pile.
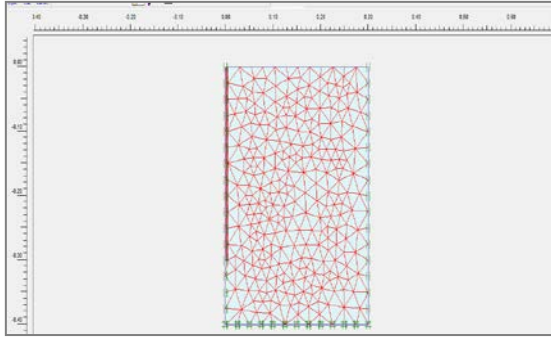
Fig.16 Pile in homogeneous soil simulation

Table 4. Properties of pile and soil in FEM

| Case	D (cm)	L (cm)	C (kN/m²)	ϕ (°)	E_{soil} (kN/m²)	E_{pile} (kN/m²)
1	0.6	30	1	30.78	1500	6.89×10^7
2	0.8	30	1	30.78	1500	6.89×10^7
3	1.0	30	1	30.78	1500	6.89×10^7
4	1.2	30	1	30.78	1500	6.89×10^7
5	1.0	20	1	30.78	1500	6.89×10^7
6	1.0	25	1	30.78	1500	6.89×10^7
7	1.0	35	1	30.78	1500	6.89×10^7
8	1.0	30	1	20.78	1500	6.89×10^7
9	1.0	30	1	25.78	1500	6.89×10^7
10	1.0	30	1	35.78	1500	6.89×10^7
11	1.0	30	1	30.78	500	6.89×10^7
12	1.0	30	1	30.78	1000	6.89×10^7
13	1.0	30	1	30.78	2000	6.89×10^7
14	1.0	30	1	30.78	1500	6.89×10^5
15	1.0	30	1	30.78	1500	6.89×10^6
16	1.0	30	1	30.78	1500	6.89×10^8
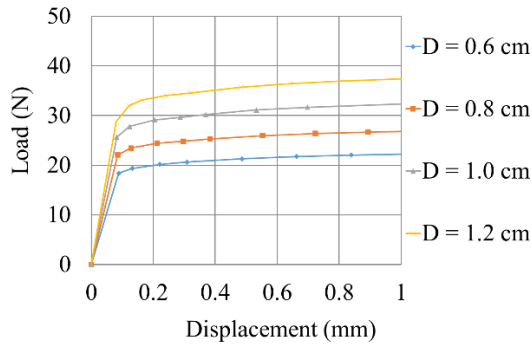
Fig.17 Total pile load with changing pile diameter
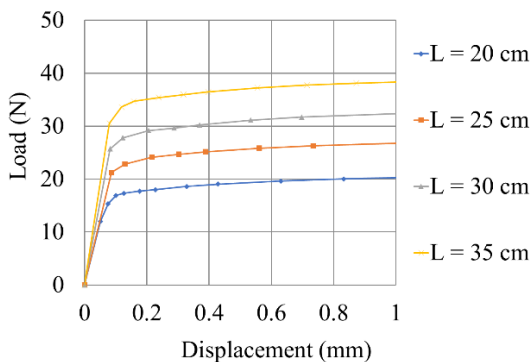

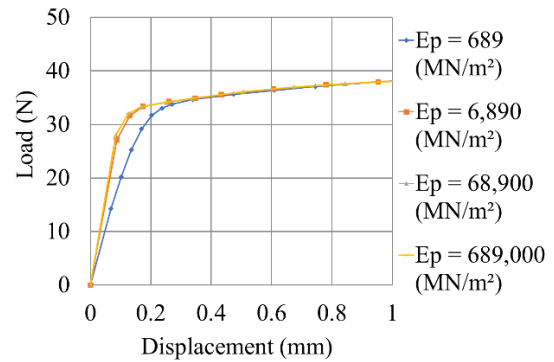Fig.18 Total pile load with changing pile length

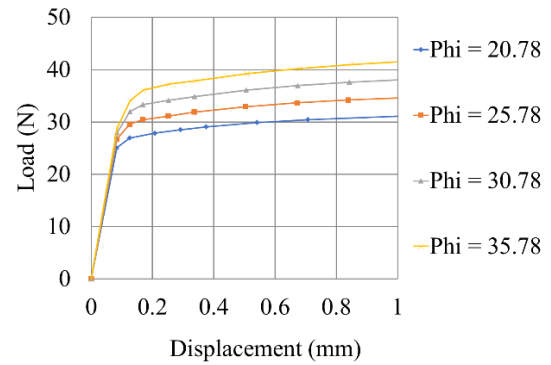Fig.19 Total pile load with changing pile modulus

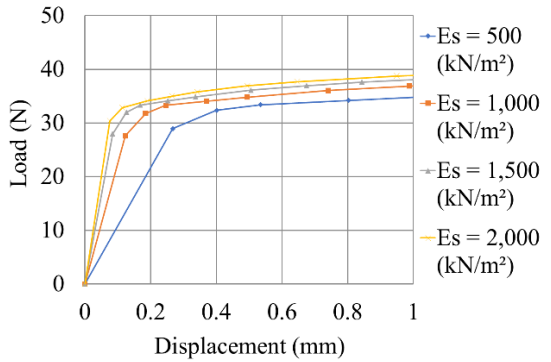Fig.20 Total pile load with changing angle of internal friction of soil

Fig.21 Total pile load with changing soil modulus

The soil properties were considered based on the internal friction angle of the soil and the soil modulus. The results showed that when the internal friction angle of the soil changed, the slope curve did not change. Therefore, the internal friction angle of the soil did not affect k_p. The modulus of the soil varied with the slope, with a higher soil modulus linked to a higher k_p.

The above results from the finite element analysis showed that k_p was independent of soil strength but was dependent on soil modulus. However, the physical model test showed that k_p increased with soil strength due to the nature of the soil and the modulus and strength of the soil were related [19]. Thus, when the strength of the soil increased, the modulus of the soil increased.

Because the modulus test is more complicated than the strength test, in practice, k_p may be obtained in relation to soil strength.

7. CONCLUSIONS

The outcomes from this research can be summarized as follows.

The simulation test with aluminium piles had less skin frictional forces than for concrete piles. The ratio between the angle of internal friction of concrete and soil to the angle of internal friction of aluminium and soil was 1.357 times.

From the physical model test of pile loading in Bangkok sandy soils and the other soil types in this test, the behavior of the skin friction of the pile was nonlinear with elastic-perfectly plastic pattern. The end bearing was nonlinear with elastoplastic-strain hardening. When incorporated into the total pile load, the piles in the soil were nonlinear with elastoplastic-strain hardening.

The determination of k_p may be considered only in the first linear elastic phase, where the displacement is not more than 10% of the pile diameter. From the FEM study, it was found that k_p depends on the pile diameter, pile length, modulus of piles, and modulus of soil, but does not depend on the soil strength. However, natural soils have soil strength relative to the soil modulus. Therefore, k_p can be considered relative to the soil strength.

8. ACKNOWLEDGMENTS

9. REFERENCES

[1] Mali S. and Singh B., Behavior of Large Piled-Raft Foundation on Clay Soil, Ocean Engineering, Vol. 149, 2018, pp. 205-216.

[2] Rabiei M. and Choobbasti A. J., Piled Raft Design Strategies for High Rise Buildings, Geotechnical and Geological Engineering, Vol. 34, Issue 1, 2016, pp. 75-85.

[3] Hoang L. and Matsumoto T., Time-Dependent Behaviour of Piled Raft Foundations on Saturated Clay: Experimental Investigations, International Journal of GEOMATE, Vol. 18, Issue 66, 2020, pp. 1-8.

[4] Katzenbach R., Arslan U., and Moormann C., Piled Raft Foundation Projects in Germany, H.

J.A. (Ed.), Design applications of raft foundations, 2000, pp. 323-391.

[5] Poulos H. G., Small J. C., and Chow H., Piled Raft Foundations for Tall Buildings, Geotechnical Engineering, Vol. 42 Issue 2, 2011, pp. 78-84.

[6] Quang H. T., Amornfa K., and Tuan T.V., Piled Raft - An Effective Foundation Design Method for High-Rise Buildings in Ho Chi Minh City, Vietnam, International Journal of GEOMATE, Vol. 21, Issue 87, 2021, pp. 102-109.

[7] Watcharasawe K., Kitiyodom P., and Jongpradist P., 3-D Numerical Analysis of Consolidation Effect on Piled Raft Foundation in Bangkok Subsoil Condition, International Journal of GEOMATE, Vol. 12, Issue 31, 2017, pp. 105-111.

[8] Amornfa K., Phienwej N., and Kitpayuck P., Current Practice on Foundation Design of High-Rise Buildings in Bangkok, Thailand, Lowland Technology International, Vol. 14 Issue 2, 2012, pp. 70-83.

[9] Szymkiewicz F., Sanagawa T., and Nishioka H., Static Pile Load Test: International Practice Review and Discussion about The European and Japanese Standards, International Journal of GEOMATE, Vol. 18 Issue 66, 2020, pp. 76-83.

[10] Szymkiewicz F., Minatchy C., and Reiffsteck P., Static Pile Load Tests: Contribution of The Measurement of Strains by Optical Fiber, International Journal of GEOMATE, Vol. 20, Issue 81, 2021, pp. 44-51.

[11] Teng W.C., Foundation Design, New Jersey: Prentice-Hall, Inc., 1962, pp. 1-466.

[12] ATC, Seismic Evaluation and Retrofit of Concrete Buildings, ATC-40 report, California, Applied Technology Council, 1996, pp. 1-345.

[13] Kiattivisanchai S., Evaluation of Seismic Performance of an Existing Medium-Rise Reinforced Concrete Frame Building in Bangkok, Master thesis, Asian Institute of Technology, 2001.

[14] Masanou P. and Amornfa K., Prediction Equation of Pile Spring Stiffness for Bored Piles in Bangkok, Journal of Engineering and Innovative, Vol. 15, Issue 2, 2022, pp.37-47.

[15] El-Garhy B., Galil A. A., Youssef A., and Raia, M. A., Behavior of Raft on Settlement Reducing Piles: Experimental Model Study, Journal of Rock Mechanics and Geotechnical Engineering, Vol. 5, Issue 5, 2013, pp. 389-399.

[16] He S., Lai J., Li Y., Wang K., Wang L., and Zhang W., Pile Group Response Induced by Adjacent Shield Tunnelling in Clay: Scale Model Test and Numerical Simulation, Tunnelling and Underground Space Technology, Vol. 120, 2022.

[17] Amornfa K., Quang H.T., and Tuan T.V., 3D Numerical Analysis of Piled Raft Foundation for Ho Chi Minh City Subsoil Conditions, Geomechanics and Engineering, Vol. 29, Issue 2, 2022, pp. 183–192.

[18] Amornkun C., Engineering Subsoil Database of Lower Central Plain, Thailand, Master thesis, Kasetsart University, Bangkok, 2010.

[19] Bowles J.E., Foundation Analysis and Design, McGraw-Hill, 1997, pp. 1-1207.